

Formation of an intense steady flux of cold atoms by the laser slowing of an atomic beam

V. I. Balykin, V. S. Letokhov, and A. I. Sidorov

Institute of Spectroscopy, Academy of Sciences of the USSR

(Submitted 10 October 1983)

Zh. Eksp. Teor. Fiz. **86**, 2019–2029 (June 1984)

A detailed experimental study is made of the slowing of an atomic beam by resonant laser radiation. By using the optimum configuration of the atomic and laser beams, employing intense two-frequency laser radiation, and limiting the velocity diffusion, one can obtain an intense steady flux of atoms with an effective temperature as low as 1 K. The intensity of the slowed atomic beam at a temperature of 1 K exceeds the intensity of the original atomic beam by a factor of $3 \cdot 10^3$.

1. INTRODUCTION

The effect of resonant laser radiation on the translational state of atoms is a problem of considerable current interest. One of the main reasons for this interest is the possibility of developing methods of controlling the spatial motion of free neutral atoms with the forces of resonant laser radiation pressure (see reviews^{1,2}). Of particular interest is the possibility of arranging a radiative slowing of atomic beams to obtain monoenergetic atomic beams with an effective temperature $T_{\text{eff}} \ll 1$ K, which is three or four orders of magnitude lower than the temperature of the source of the atomic beam.

A number of experiments taking different approaches to the problem have already been done. The first reports^{3,4} of the slowing of an atomic beam demonstrated that a pulsed slowing of an atomic beam can be arranged by scanning the laser frequency to follow the change in the velocity of the atoms. The possibilities of this method are limited because of the loss of cyclicity of the interaction of the atoms with the laser radiation. Another method of radiative slowing of an atomic beam, this one capable of yielding a steady flux of cold atoms, is the counter-illumination of the atomic beam by resonant laser radiation of high intensity and fixed frequency, tuned to within the absorption line of the atomic beam. This method has succeeded⁵ in compressing the velocity distribution of an atomic beam to a relative-motion temperature of 1.5 K.

The subsequent development of a method of continuous fine tuning of the laser frequency to the frequency of the resonant transition enabled the authors of Refs. 6 and 7 to obtain slowed atomic fluxes of low intensity, with an effective temperature as low as 0.07 K.

For real physical experiments with beams of cold atoms, beam intensity is an important parameter. With the intention of using cold atoms in a number of future experiments, in the present study we investigated the problem of obtaining an intense steady flux of cold atoms.

This work was a continuation of our previous studies⁵ and was intended to produce two main results: a) to produce an atomic beam with a low effective temperature; b) to achieve a high intensity of the beam of slowed atoms.

It has been pretty well ascertained theoretically (see Ref. 1) that all the main features of the motion of an atom in a resonant field are due to two main causes: a) the force of

radiation pressure and its dependence on the velocity of the atom; b) quantum fluctuations in the force of radiation pressure. The force of radiation pressure is capable in principle of gathering the atoms into a narrow velocity group around zero velocity from an appreciable part of the velocity distribution of the atomic beam. The limiting width of the velocity distribution will be given by the expression⁸ $\delta v \approx (\hbar\gamma/M)^{1/2}$, where γ is the half-width of the absorption line and M is the mass of the atom, and the corresponding effective temperature is equal to 10^{-2} – 10^{-3} K. The quantum fluctuations of the force of radiation pressure have up till now been considered mainly from the standpoint of their effect on the minimum possible temperature of the cooled beams. The width of the velocity distribution near the turning point of the slowed atoms reaches a value $\Delta v \approx (\hbar\Omega/M)^{1/2}$, where Ω is the frequency detuning of the light wave from the frequency of the atomic transition.⁹ The corresponding effective temperature is 10^{-1} – 10^{-2} K.

More important from a practical standpoint, however, is the influence of the quantum fluctuations of the force of radiation pressure (we shall hereafter refer to these fluctuations as the velocity diffusion of the atoms) on the transverse spatial distribution of the atoms in the beam. For a prolonged interaction of an atom with the retarding field a slight increase in the perpendicular velocity of the atom leads to a noticeable displacement of the atom in the transverse direction, with the result that the atom can move out of the laser beam and cease to be acted upon by the retarding force of radiation pressure. It is clear from qualitative considerations that the configuration of the laser beam and the interaction time and length can be optimized to ensure simultaneously both a low effective temperature of the atomic beam and a high beam intensity.

In the present study we investigate experimentally the evolution of both the longitudinal and transverse velocity distributions of an atomic beam interacting with an intense resonant laser beam. On the basis of our measurements we study the influence of the diffusion of the atoms in velocity space on the formation of an intense cooled atomic beam, and we obtain such beams with temperatures down to 1 K.

2. EXPERIMENTAL METHOD AND APPARATUS

The experimental arrangement was analogous to that used in our previous study.⁵ Let us briefly recall the main

elements of this arrangement and discuss the changes made for the present study. A thermal beam of sodium atoms was illuminated by three laser beams. One of them (the intense laser beam) was directed counter to the atomic beam and caused a deformation of the velocity distribution. The frequency of the radiation in this beam was set within the Doppler width of the absorption line of the atomic beam and held fixed. The emission spectrum of the intense laser consisted of two axial modes, with a frequency difference between them equal to the hyperfine splitting of the ground state of the sodium atom (1772 MHz). The second and third laser beams were formed by splitting the beam of a single-mode cw dye laser into two beams. The two beams intersected the atomic beam at the end of the interaction zone. One of them crossed the atomic beam at a small angle and detected the longitudinal velocity distribution, while the other beam was perpendicular to the atomic beam and measured the transverse spatial distribution. The longitudinal velocity distribution was recorded by tuning the frequency of the single-mode laser over the Doppler contour of the absorption line and simultaneously detecting the fluorescence signal. The dimension of the perpendicular probe beam was smaller than the transverse dimension of the atomic beam. The transverse spatial distribution of the atomic beam was recorded by monitoring the fluorescence signal from atoms excited by the perpendicular beam as it crossed the atomic beam.

The main difference in the detection system from that used in the previous study⁵ was that both the longitudinal velocity distribution and the transverse spatial distribution were recorded after interruption of the strong field, as the laser frequency was rapidly scanned along the contour of the absorption line over a time shorter than the mean transit time of an atom through its interaction zone with the strong field. We thus recorded an instantaneous picture of the distributions of the atomic beam. By changing the delay time between the interruption of the strong field and the start of the scanning of the absorption line, we could record the evolution of the velocity distribution as a function of the time over which the atomic beam was illuminated by the strong field.

The experimental layout is shown in Fig. 1. The apparatus consists of the following main elements: two argon lasers for pumping the dye lasers, a two-frequency dye laser 2, a probe dye laser 1, a mechanical chopper 3 for interrupting the beam of the two-frequency laser, and a vacuum chamber 4 with an atomic-beam source 5. The fluorescence signal from the atoms excited by the intense beam and probe beam

was collected to the cathode of photomultiplier 6 and registered on oscilloscope 9. The geometry of the atomic beam was varied depending on the measurements to be made. The residual gas pressure in the vacuum chamber with the atomic-beam source in operation was no higher than $5 \cdot 10^{-6}$ Torr.

The spectral composition of the dye-laser emission was monitored with a scanning spherical Fabry-Perot etalon 7. The beam from the single-mode laser was split into two beams by a half-silvered mirror; one of the beams intersected the atomic beam at a small angle (4°) in the detection zone, while the other intersected a right angles. The maximum scanning rate of the single-mode laser frequency was

$$\gamma = d\Omega/dt = 3.3 \cdot 10^8 \text{ GHz/sec}$$

The Doppler width of the absorption line of the atomic beam was $\Delta\Omega \approx 1500$ MHz. At the maximum laser-frequency scanning rate the absorption line could thus be scanned in a time $\Delta t = \Delta\Omega/\gamma = 5 \cdot 10^{-4}$ sec. The width of the observable velocity peak varied in the range 70–300 MHz. The laser frequency could be scanned over such a range in a time of 50–100 μsec , which was substantially shorter than the transit time of the atoms through the detection zone. This in turn meant that the observed dependence of the fluorescence signal on the frequency of the probe laser gave a rather faithful reproduction of the instantaneous velocity distribution of the atoms in the region of the velocity peak.

The width of the absorption line of the atomic beam during probing by the perpendicular laser beam was governed by the hyperfine splitting of the excited state and by the residual Doppler broadening and amounted to around 100 MHz. The time over which the frequency of the probe laser was tuned over such a frequency interval was 30 μsec , also substantially shorter than the mean transit time of the atoms through the interaction zone. Thus the probing by the perpendicular laser beam likewise revealed the instantaneous spatial distribution of the atomic beam.

3. TIME EVOLUTION OF THE LONGITUDINAL VELOCITY DISTRIBUTION

For studying the temporal evolution of the longitudinal velocity distribution as a function of the interaction time with the intense laser beam we chose the following geometry for the atomic and laser beams (Fig. 1b). The collimation of the atomic beam was determined by the exit aperture (diameter $D_1 = 0.3$ mm) of the source and a diaphragm (diameter $D_2 = 0.3$ mm) placed a distance $L = 40$ cm from the source; the corresponding collimation angle was $\Delta\varphi = 1.5 \cdot 10^{-3}$ rad. The caustic of the laser beam was chosen such that the

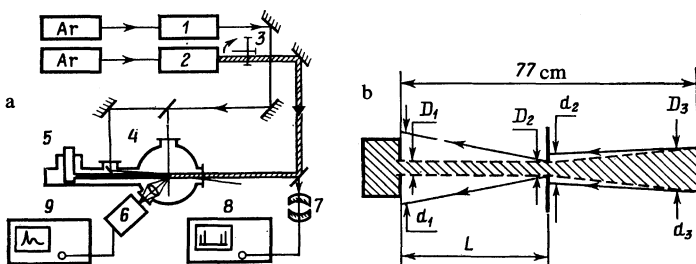


FIG. 1. a) Schematic of the experimental apparatus: Ar) argon laser, 1) single-mode probe laser, 2) two-high-power frequency laser, 3) mechanical chopper, 4) vacuum chamber, 5) source of atomic beam, 6) photomultiplier, 7) scanning Fabry-Perot etalon, 8,9) oscilloscopes. b) The geometries of the atomic (hatched region) and intense laser beams in two cases: 1) for measuring the longitudinal velocity distribution of the atoms in the beam ($D_1 = D_2 = 0.3$ mm, $D_3 = 0.8$ mm, $d_1 = 1.5$ mm, $d_2 = 0.4$ mm, $d_3 = 0.8$ mm, $L = 40$ cm); 2) for measuring the transverse spatial distribution of the atomic beam ($D_1 = D_2 = 0.3$ mm, $D_3 = 1.8$ mm, $d_1 = 0.55$ mm, $d_2 = 0.75$ mm, $d_3 = 1.9$ mm, $L = 22$ cm).

neck of the intense laser beam was located in the region of the diaphragm.

As the laser beam propagated toward the source of the atomic beam, its transverse dimension increased. The diameter of the laser beam was $d_1 = 1.5$ mm at the source of the atomic beam, $d_2 = 0.4$ mm at the diaphragm, and $d_3 = 0.8$ mm in the detection region. The use of an intense beam which diverges toward the atomic beam source made for an increase in the saturation parameter G as the atoms moved from the source to the detection zone. The force of radiation pressure has the following dependence on the saturation parameter:

$$F = -\hbar k \gamma \frac{G}{1 + G + (\Omega + kv)^2 / \gamma^2}, \quad (1)$$

where $\hbar k$ is the photon momentum, 2γ is the absorption linewidth, $\Omega = \omega_{\text{las}} - \omega_0$ is the detuning of the laser frequency ω_{las} from the transition frequency ω_0 , and $G = I_{\text{las}} / I_{\text{sat}}$ (I_{las} is the intensity of the laser beam and I_{sat} is the saturation intensity of the transition). This expression shows that as the saturation parameter increases, so does the velocity interval in which the force of radiation pressure acts efficiently on the atoms. In situations like the present case where one is attempting to produce a monoenergetic beam, the chosen geometry ensures that the retarding force of radiation pressure continues to act effectively on the atoms of the velocity peak during the formation and narrowing of the latter as the atoms move along the interaction region.

The atomic beam remained inside the laser beam throughout the entire interaction zone except at the diaphragm, where the dimensions of the laser beam and atomic beam were equal on the source side. The geometric length of the interaction zone was 77 cm. The diameter of the probe beam as it detected the longitudinal velocity distribution in the observation zone was $d_{\text{probe}} = 1.3$ mm.

Figure 2 shows the experimental dependence of the fluorescence intensity on the frequency of the probe field. The double peak on the left-hand side of the curves is an absorption line of beam atoms excited by the perpendicular laser beam and is used as a marker. The position of the higher of these two peaks corresponds to the zero of the velocity scale. The dashed curve on trace 1 corresponds to the original velocity distribution of the atomic beam. Trace 1 corresponds to the initial stage in the deformation of the velocity distribution for a 0.12-msec interaction time of the atomic beam with the intense field. The corresponding interaction length L_{int} was 10 cm. The frequency of the intense field was held fixed at a set value in resonance with atoms having an initial velocity $v_0 = 9.3 \cdot 10^4$ cm/sec. Trace 2 corresponds to an interaction time of 0.31 msec and an interaction length of 25 cm. It is seen that the velocity distribution has been compressed. The fraction of atoms in the velocity peak is about 25% of the total number of atoms in the original velocity distribution. As the interaction time is increased further the peak shifts toward lower velocities. The position of the peak on trace 6 corresponds to a velocity of $3.9 \cdot 10^4$ cm/sec.

The absolute decrease in the velocity of the atoms in the series of traces shown is $\Delta v = 5.4 \cdot 10^4$ cm/sec. It should be noted that the apparent width of the recorded velocity peaks

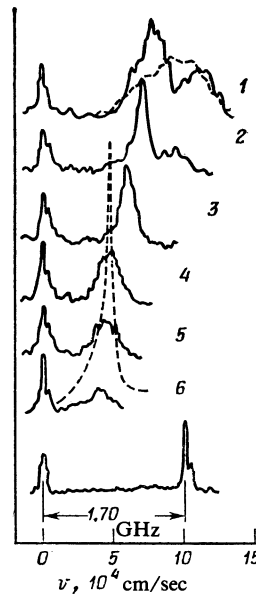


FIG. 2. Temporal evolution of the velocity distribution of the atomic beam during interaction with the intense field. The resonant velocity of the initial velocity distribution (the dashed curve in the upper trace) is $v_0 = 9.3 \cdot 10^4$ cm/sec. The peak velocities v at various values of t and L_{in} are: 1) $L_{\text{in}} = 10$ cm, $t = 0.12$ msec, $v = 7.9 \cdot 10^4$ cm/sec; 2) $L_{\text{in}} = 25$ cm, $t = 0.31$ msec, $v = 7.1 \cdot 10^4$ cm/sec; 3) $L_{\text{in}} = 45$ cm, $t = 0.62$ msec, $v = 6 \cdot 10^4$ cm/sec; 4) $L_{\text{in}} = 57$ cm, $t = 0.84$ msec, $v = 4.7 \cdot 10^4$ cm/sec; 5) $L_{\text{in}} = 59$ cm, $t = 0.9$ msec, $v = 4.3 \cdot 10^4$ cm/sec; 6) $L_{\text{in}} = 66$ cm, $t = 1.08$ msec, $v = 3.9 \cdot 10^4$ cm/sec.

is greater than the true width and is due to the insufficiently rapid frequency scanning of the probe field.

Figure 3 shows the experimental and theoretical average velocity of the narrowed velocity peak as a function of the interaction length with the intense field under the conditions of our experiment. The solid curve was calculated for the power and configuration of the intense field used in the measurements. The dashed curves were obtained under the assumption that the pressure of radiation having an acceleration $4 \cdot 10^7$ cm/sec² and various initial velocities slowed down all the atoms equally. The experimental points were obtained in three series of measurements; the filled circles correspond to the data of Fig. 2. Comparison of the experimental and calculated curves implies that the diverging-in-

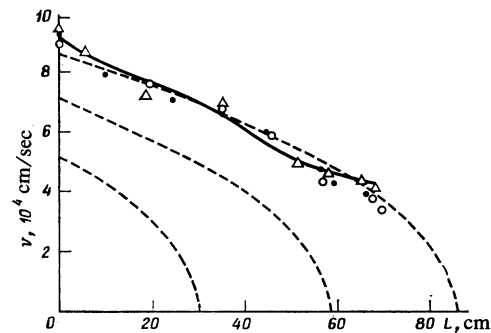


FIG. 3. Velocity of the peak arising in the velocity distribution as a function of the length of interaction with the intense laser beam: \triangle , \circ , and \bullet are the results of the three series of measurements, the solid curve was calculated for the power and configuration of the intense field used in the experiment, and the dashed curves were calculated for a constant atomic acceleration $a = -4 \cdot 10^7$ cm/sec² and for various initial velocities.

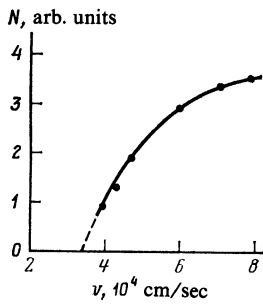


FIG. 4. Relative density of atoms in the peak of the compressed velocity distribution versus the average velocity of the peak during the slowing; $v_0 = 9.3 \cdot 10^4$ cm/sec.

tense-beam configuration used in the experiment provides an efficient slowing of the atoms, with an acceleration equal to 40% of the maximum possible value (which is achieved in a two-level Na atom with an excited-state lifetime $\tau = 16$ nsec and at a laser-beam intensity $I \gg I_{\text{sat}}$).

Together with the slowing down, i.e., the shift of the velocity peak toward zero, the velocity distributions (Fig. 2) show a marked decrease in the fraction of the atoms in the peak. Figure 4 shows the relative concentration of atoms in the velocity peak as a function of their average velocity as they are decelerated. It is seen that the fraction of atoms in the peak falls off sharply as the velocity reaches about $3 \cdot 10^4$ cm/sec. There are three effects that could potentially contribute to this decrease in the number of slowed atoms: 1) scattering of the atoms by the residual gas; 2) geometric spreading in the transverse direction; 3) diffusive transverse spreading. Let us discuss the contribution of each of these effects.

To estimate the effect of the scattering of atoms by the residual gas we measured the attenuation of the original atomic beam as a function of the pressure in the chamber. From these measurements we determined the mean free path of the atoms to be $\langle \lambda \rangle_{v_0} = 190$ cm. Knowing this value, we could determine the dependence of the mean free path on the velocity of the atoms.¹⁰ It was thus found that a decrease in the velocity of the atoms from $v_0 = 9.3 \cdot 10^4$ cm/sec to $3.9 \cdot 10^4$ cm/sec should lead to no more than a 20% attenuation in the intensity of the atomic beam. In the experiment, however, the amplitude of the peak decreased by a factor of 3.8.

The next factor influencing the amplitude of the velocity peak is the geometric spreading of the beam atoms. The diameter of the atomic beam at the end of the interaction zone on account of the geometric spreading of the atoms during the velocity compression of the beam is given by

$$\Delta d_{\text{geom}} = \Delta \varphi v_0 t_{\text{tr}},$$

where $\Delta \varphi = 1.5 \cdot 10^{-3}$ rad is the initial divergence of the atomic beam, $v_0 = 7.9 \cdot 10^4$ cm/sec is the initial average velocity of the atoms, and t_{tr} is the transit time of the decelerating atoms through the interaction region; the transit time is the sum of the time $t_{\text{ill}} = 1.08 \cdot 10^{-3}$ sec during which the atom is illuminated by the intense field over a length $L_{\text{int}} = 66$ cm and the time $t_{\text{tr}}^{\text{fr}}$ required for the free transit of the remaining distance to the observation region (11 cm) at the decreased velocity $v = 3.9 \cdot 10^4$ cm/sec. The total transit

time is $t_{\text{tr}} = t_{\text{ill}} + t_{\text{tr}}^{\text{fr}} = 1.36 \cdot 10^{-3}$ sec and, consequently, the increase in the diameter of the atomic beam on account of geometric spreading is $\Delta d_{\text{geom}} = 1.2$ mm. This value is smaller than the diameter of the probe laser beam $d_{\text{probe}} = 1.3$ mm. Therefore, the transverse geometric spreading of the atoms is not responsible for the decrease in the intensity of the peak in the velocity distribution.

Let us now estimate the influence of diffusion on the transverse spatial distribution of the atomic beam. We assume for simplicity that the scattering of light by an atom is isotropic. Then, after the scattering of n photons the transverse velocity distribution $f(v_{\perp})$ of an atom having an initial transverse velocity $v_0 \Delta \varphi / 2$ is of the form¹¹

$$f(v_{\perp}) \propto \exp[-(v_{\perp} - v_0 \Delta \varphi / 2)^2 / 2v_{\text{rec}}^2 (N/3)], \quad (2)$$

where v_0 is the longitudinal velocity of the atom, $v_{\text{rec}} = \hbar k / M$ is the recoil velocity, $\Delta \varphi$ is the angular divergence of the atomic beam, and $k = 2\pi/\lambda$. It follows from expression (2) that the maximum transverse velocity of the atom is:

$$v_{\perp}^{\text{max}} = 1/2 v_0 \Delta \varphi + v_{\text{rec}} (2/3 N)^{1/2}.$$

Accordingly, the transverse dimension of the atomic beam with allowance for velocity diffusion is given by the expression

$$d_{\text{diff}} = \int_0^{t_{\text{ill}}} v_{\perp}^{\text{max}}(t) dt. \quad (3)$$

The configuration of the intense laser beam provided an almost uniform slowing of the atoms. Under this assumption the number of reradiated photons is

$$N = |a| t_{\text{ill}} (h/M\lambda)^{-1}, \quad (4)$$

where a is the acceleration of an atom. Then the increase in the transverse dimension of the atomic beam on account of the diffusion of the atoms is given by the expression

$$\Delta d_{\text{diff}} = 2 \left(\frac{8}{27} a h / M \lambda \right)^{1/2} t_{\text{ill}}^{3/2}. \quad (5)$$

Under our experimental conditions, viz., $t_{\text{ill}} = 1.08$ msec and $a = -4 \cdot 10^7$ cm/sec², the increase in the diameter on account of diffusion is $\Delta d_{\text{diff}} = 4.1$ mm. Then the total diameter of the beam is $d = \Delta d_{\text{diff}} + d_3 = 5.3$ mm. The power of the probe laser beam, equal to 1 mW at a beam diameter of 1.3 mm, corresponds to a six-fold saturation of the resonance transition, while the effective diameter within which the fluorescence signal was detected was $d_{\text{fl}} = 2$ mm. The fluorescence signal from the probe field is proportional to the volume from which the photons are collected. The decrease in the fluorescence signal due to the diffusive spreading of the atoms is thus by a factor of $d_{\text{diff}}^2 / d_{\text{fl}}^2 \approx 7$. The dashed curve on trace 6 in Fig. 2 shows the compression of the velocity distribution of the atomic beam as calculated without allowance for diffusion. The ratio of the amplitudes of the calculated velocity peak to that of the experimentally measured peak is equal to 11, in rather good agreement with the above estimate.

Our analysis of the various effects thus shows that the sharp decrease observed in the number of slowed atoms, i.e., in the intensity of the peak in the velocity distribution, is attributable to the transverse diffusion of the atoms in the course of their interaction with the intense laser beam.

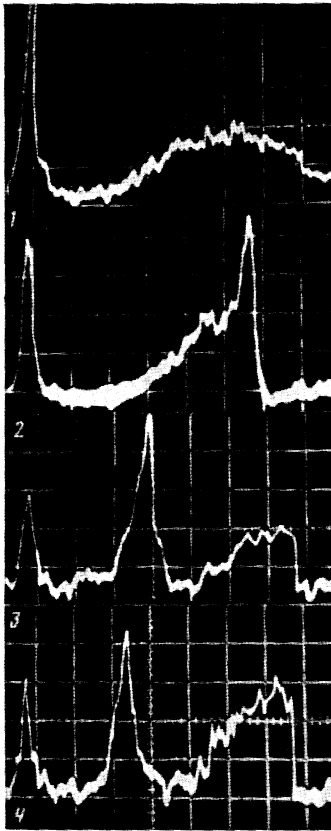


FIG. 5. Observation of compression of the velocity distribution of an atomic beam under the action of intense resonant laser radiation: 1) oscilloscope trace of the velocity distribution in the atomic beam; the peak at the left indicates the zero-velocity position; 2,3,4) deformed velocity distributions at resonances of the laser beam with atoms in the high-velocity region (2), with atoms having the most probable velocity (3), and with the low-velocity atoms (4).

The influence of the diffusion of atoms on their slowing down was checked experimentally in the following way. The configuration of the atomic and intense laser beams was modified from the case described above (see Fig. 1b) to give a strong compression of the velocity distribution of the atomic beam in the initial short atom-field interaction region in front of the diaphragm. For this purpose the source and diaphragm had the same apertures as before, but the distance between them was shortened to $L = 22$ cm, at an overall distance between the source and the detection zone of 77 cm. The characteristic dimensions of the strong field were $d_1 = 0.55$ mm at the source, $d_2 = 0.75$ mm at the diaphragm, and $d_3 = 1.9$ mm in the detection region. This configuration of the field in fact gave a strong compression of the velocity distribution of the atomic beam, as is seen in the oscilloscope traces in Fig. 5, without sharply attenuating the beam intensity. Between the second diaphragm (d_2) and the interaction zone the velocity distribution changed slightly (Fig. 6) as a result of a decrease in the saturation parameter and a shift of the velocity peak away from exact resonance with the field. In an independent experiment we observed some broadening of the transverse spatial distribution of the beam atoms as a result of their diffusion.

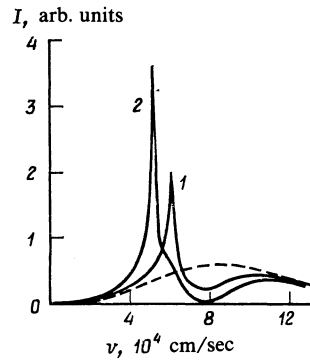


FIG. 6. Calculated compression of an atomic beam under the experimental conditions for different interaction lengths of the beam with the intense laser field: 1) $L_{in} = 22$ cm, 2) $L = 77$ cm. The dashed curve shows the original velocity distribution.

4. FORMATION OF AN INTENSE FLUX OF SLOW ATOMS

Our measurements of the longitudinal velocity and transverse spatial distributions have shown that in order to obtain atomic beams with low velocities (a low effective temperature) and a high density it is necessary to diminish the influence of diffusion on the transverse spreading of the atoms. A natural possibility for decreasing this parasitic effect is to decrease the number of reradiated photons, and that, in turn, dictates a switch to the slowing of beams having lower initial velocities.

Let us estimate the value of the initial velocity which would yield atoms with zero velocity at an acceptable loss of atoms upon cooling on account of their diffusion in the laser slowing process. The decrease in the density of atoms during their slowing is given by the simple relation $\alpha = (d_{diff}/d_{las})^2$, where d_{las} is the diameter of the intense laser beam. Assuming that, as in our experiment, the atoms are slowed uniformly in the intense field and using formula (5), we obtain for the slowing of the velocity

$$\Delta v = \left[\frac{\alpha (a d_{las})^2}{32 h / 27 M \lambda} \right]^{1/3} \quad (6)$$

If we consider $\alpha = 10$ to be an acceptable decrease in the beam density due to diffusion and take $d_{las} = 0.1$ cm and $a = 9.1 \cdot 10^7$ cm/sec², we obtain the required value of the slowing as $\Delta v = 6.2 \cdot 10^4$ cm/sec. At the acceleration realized in the experiment in which we measured the longitudinal velocity distribution, viz., $a = 4 \cdot 10^7$ cm/sec², the required initial value of the velocity is $3.6 \cdot 10^4$ cm/sec. The experimental measurements (see Fig. 4) also confirm that a decrease in the absolute velocity of the atoms by an amount $\Delta v = 5 \cdot 10^4$ cm/sec leads to a decrease in the density by no more than one order of magnitude.

Taking all these estimates into account, we chose the following experimental procedure. The frequency of the laser field was set at resonance with atoms having an initial velocity of $5.5 \cdot 10^4$ cm/sec. For the case when the laser beam has a diverging caustic which ensures an almost uniformly decelerated motion of the atoms, the position of the frequency determines the length of the interaction zone: here $L_{int} = 31$ cm. The neck of the laser beam was located in the detection zone, and the diameter of the beam at this place

was $d_3 = 0.7$ mm. The collimation of the atomic beam, $\Delta\varphi = 1.05 \cdot 10^{-2}$ rad, was determined by the exit aperture in the source ($D_1 = 1$ mm) and the aperture in the diaphragm ($D_2 = 1$ mm), which was located a distance of 19 cm from the source. The diameter of the laser beam was $d_2 = 1.1$ mm at the diaphragm and $d_1 = 1.3$ mm at the atomic-beam source (after passing through the diaphragm). The laser radiation had a power of 400 mW, giving a saturation parameter of $G_3 = 10\,400$ in the detection zone and $G_1 = 550$ in the region of the atomic-beam source. The former value of the saturation parameter provides an effective slowing of atoms with an initial velocity of

$$\Delta v = \lambda \gamma (1 + G_3)^{1/2} = 3 \cdot 10^4 \text{ cm/sec.}$$

The probe field was directed along the atomic beam rather than counter to it as in the previous measurements, and it intersected the atomic beam at an angle of 4° . Having both the atomic beam and the probe laser beam going in the same direction enabled us to avoid the simultaneous detection of the fluorescence from the slow atoms at the probed transition $3S_{1/2}(F=2) \rightarrow 3P_{3/2}(F'=3)$ and from the fast atoms at the transition $3S_{1/2}(F=1) \rightarrow 3P_{3/2}(F'=1,2)$, since the Doppler shift of the atomic beam is approximately equal to the frequency difference between these two transitions.

Figure 7 shows the experimentally measured velocity distributions of the atomic beam in the slow-velocity region. Curve 1 is the original velocity distribution, while curve 2 is the velocity distribution formed as a result of the interaction with the strong field. By comparing the two curves we see that the laser slowing of the atomic beam produces an intense flux of slow atoms with an effective temperature of around 1 K. Figure 8 shows the enhancement of the fraction of cold atoms during the laser slowing of the atomic beam. At a temperature of 1 K the intensity of the beam of cold atoms reaches 10^4 times that of the thermal atomic beam (curve 1). In the experiment the number of beam atoms with such low effective temperatures (the slow atoms) is significantly smaller because of their unavoidable scattering at the high density of the atomic beam itself near the exit aperture of the source. Curve 2 shows the enhancement of the fraction of atoms for the actual atomic beam used in the experiment.

Unfortunately, we could not reliably detect the slower atoms in the experiment because of the overlap of the flu-

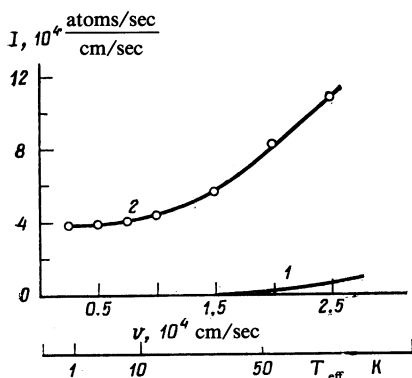


FIG. 7. Velocity distribution of the cooled atomic beam in the slow-velocity region: 1) original distribution; 2) deformed velocity distribution.

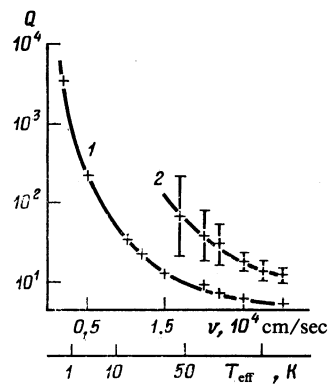


FIG. 8. Intensity enhancement Q of the atomic beam in the low-velocity region during its slowing by the laser field: 1) curve obtained under the assumption that the atomic beam has a thermal velocity distribution; 2) for the original velocity distribution measured in the experiment.

orescence signals from the parallel beam and from the perpendicular beam used for calibrating the frequency scale. By spatially separating the points of intersection of these beams with the atomic beam and using spatially separate detection of the fluorescence signals, one could detect colder atoms.

5. CONCLUSION

In this paper we have reported the first detailed experimental study of the slowing of an atomic beam by resonant laser radiation and the formation of a steady flux of cold sodium atoms. It was found that the main limitation in a real one-dimensional experiment is the diffusion of atoms in velocity space; such a diffusion is unavoidable in radiative cooling and causes a transverse spatial diffusion of the atoms. By using the optimum configuration of the atomic and laser beams and employing intense two-frequency laser radiation with a frequency fixed within the absorption line, one can obtain an intense steady flux of atoms with an effective temperature as low as 1 K. The method we have developed for obtaining cold atoms makes possible a number of interesting experiments. First, one can inject cold atoms into a laser trap and optically confine them.^{1,2} Second, the slowed atoms can be used to obtain extremely narrow spectral resonances with widths of several Hz.

In closing, we wish to thank V. G. Minogin for a helpful discussion of the results.

¹V. A. Letokhov and V. G. Minogin, Phys. Rep. **73**, 1 (1981).

²A. Ashkin, Science **210**, 1081 (1980).

³V. I. Balykin, V. S. Letokhov, and V. I. Mishin, Pis'ma Zh. Eksp. Teor. Fiz. **29**, 614 (1979) [JETP Lett. **29**, 560 (1979)].

⁴V. I. Balykin, V. S. Letokhov, and V. I. Mishin, Zh. Eksp. Teor. Fiz. **78**, 1376 (1980) [Sov. Phys. JETP **51**, 692 (1980)].

⁵S. V. Andreev, V. I. Balykin, V. S. Letokhov, and V. G. Minogin, Pis'ma Zh. Eksp. Teor. Fiz. **34**, 463 (1981) [JETP Lett. **34**, 442 (1981)]; Zh. Eksp. Teor. Fiz. **82**, 1429 (1982) [Sov. Phys. JETP **55**, 828 (1982)].

⁶W. D. Phillips and H. Metcalf, Phys. Rev. Lett. **48**, 596 (1982).

⁷J. V. Prodan, W. D. Phillips, and H. Metcalf, Phys. Rev. Lett. **49**, 1149 (1982).

⁸I. V. Krasnov and N. Ya. Shaparev, Zh. Eksp. Teor. Fiz. **77**, 899 (1979); **79**, 391 (1980) [Sov. Phys. JETP **50**, 453 (1979); **52**, 196 (1980)].

⁹T. V. Zueva, V. S. Letokhov and V. G. Minogin, Zh. Eksp. Teor. Fiz. **81**, 84 (1981) [Sov. Phys. JETP **54**, 38 (1981)]; Opt. Commun. **38**, 225 (1981).

¹⁰N. F. Ramsey, Molecular Beams, Clarendon Press, Oxford (1956).

¹¹A. Ishihara, Statistical Physics, Academic Press, New York (1971).

Translated by Steve Torstveit